J. Mol. Biol. (1993) 234, 357–372

Domain Closure in Lactoferrin

Two Hinges Produce a See-saw Motion Between Alternative Close-packed Interfaces

Mark Gerstein[1,2], Bryan F. Anderson[3], Gillian E. Norris[3] Edward N. Baker[3], Arthur M. Lesk[4] and Cyrus Chothia[1,5]

[1]*MRC Laboratory of Molecular Biology Hills Road, Cambridge CB2 2QH, U.K.*

[2]*Department of Chemistry, Cambridge University Lensfield Road, Cambridge CB2 1EW, U.K.*

[3]*Department of Chemistry and Biochemistry Massey University, Palmerston North, New Zealand*

[4]*Department of Haematology, Cambridge University Hills Road, Cambridge CB2 2QH, U.K.*

[5]*Cambridge Center for Protein Engineering Hills Road, Cambridge CB2 2QH, U.K.*

(Received 17 December 1992; accepted 21 April 1993)

Lactoferrin is an iron transport protein. Upon binding iron, the two domains in the N-terminal half of the molecule move together. Previous work has shown that this domain closure involves two hinges. Using the newly refined structure of the open form, the structural mechanism underlying this motion is analyzed here in detail.

Upon closure the domains rotate 54° essentially as rigid bodies. The axis of rotation passes through the two β-strands linking the domains. These strands contain hinges in the sense that three large torsion angle changes are responsible for the bulk of the motion while smaller torsion angle changes in neighboring residues are responsible for the remainder of the motion. The rotation axes of these three torsion angle changes are nearly parallel to the axis of the overall 54° rotation, so the local motion in the hinges can be directly related to the overall motion.

A crucial feature of the hinge residues is that they have very few packing constraints on their main-chain atoms.

The domains make different packing contacts with each other in the open and closed forms. These contacts form two interdomain interfaces arranged on either side of the hinges. Pivoting about the hinges produces a see-saw motion between the two interfaces. That is, when the domains close down, residues in the interface on one side of the hinges become buried and close-packed and residues on the other side become exposed. The situation is reversed when the domains open up.

Lactoferrin provides a particularly clear example of the general features of hinged domain motion. It is compared to other instances of hinged domain closure and contrasted with instances of shear domain closure, where the overall motion is a summation of many small sliding motions between close-packed segments of polypeptide.

Keywords: macromolecular structure; protein dynamics; conformational change; helix shear motion; binding proteins

1. Introduction

Large movements of one protein domain relative to another are important for the function of many proteins (Anderson *et al.*, 1979; Janin & Wodak, 1983; Bennett & Huber, 1984). They are involved in the transport of metabolites and in cellular motion. They also play a crucial role in the catalytic

0022-2836/93/220357-16 $08.00/0

mechanisms of certain enzymes: in shielding the substrate from water, surrounding it with catalytic residues, and preventing the escape of kinetic intermediates (Anderson *et al.*, 1979; Knowles, 1991).

For fast low-energy transitions, proteins must maintain well-packed interiors and interfaces that do not have steric clashes or large cavities. How can a protein accommodate large domain movements while still maintaining its packing? Shear motions provide one possible structural mechanism (Chothia *et al.*, 1983; Lesk & Chothia, 1984; Chothia & Lesk, 1985; Rojewka & Elber, 1990; McPhalen *et al.*, 1992). These involve small (1 to 2 Å) sliding movements between close-packed segments of polypeptide, e.g. helices. The culmination of many shear movements both within and between domains can result in a large overall movement.

Hinge mechanisms provide an alternate way for protein domains to move while still maintaining their packing. Domains can move as rigid bodies with all the deformations confined to linking hinge regions. Such motions require different interfaces from those found for shear motions. Good structural evidence for such mechanisms was provided by the recent structure determination and analysis of the open and closed forms of the iron transport protein lactoferrin (Anderson *et al.*, 1990) and the large variant of adenylate kinase (Schulz *et al.*, 1990; Gerstein *et al.*, 1993).

Lactoferrin is particularly well-suited to studies of hinged domain motion because well-refined high-resolution structures of the open and closed forms are available. Certain features of the domain closure in lactoferrin have been described previously (Anderson *et al.*, 1990; Baker *et al.*, 1991). Here, by comparison of open and closed forms of lactoferrin that work is extended. The hinged mechanism for domain closure in lactoferrin is contrasted with the shear mechanisms in other proteins. Attention is focussed on two questions: (1) how is the overall motion of the two domains related to the torsion angle changes in the hinges; and (2) how does the packing and interface structure accommodate large deformations in the hinges?

2. The Structure of Lactoferrin

The structure of lactoferrin has been determined by X-ray crystallography (Anderson *et al.*, 1987, 1989, 1990; Norris *et al.*, 1991). The molecule is divided into N-terminal and C-terminal lobes, which have clear sequence homology and must have arisen from a gene duplication. Each lobe contains two domains, denoted N1 and N2 and C1 and C2. Within each lobe the domains are covalently linked by two strands of antiparallel β-sheet (Fig. 1), and at the interface between the domains there is an iron binding site. Each domain, in turn, has an α/β structure (Levitt & Chothia, 1976), containing a central β-sheet with helices packed on both faces. (Residue numbering is given in Table 1.)

Crystal structures have been determined for an iron-bound form and for an iron-free form. In the iron-bound form (Anderson *et al.*, 1989), N1 and N2 are closed together with an iron atom bound between them. The same is true for C1 and C2.

In the iron-free form (Anderson *et al.*, 1990), N1 and N2 are separated, exposing a deep cleft between them. Baker *et al.* (1991) have shown that the domains move as almost rigid bodies and that the major conformational change occurs in "hinge" regions on the two strands that link the domains. The hinges are approximately between Thr90 and His91 on strand e and between Val250 and Pro251 on strand j. Although C1 and C2 have also lost their iron ligand, they show no appreciable conformational change and are still closed together. The absence of changes in the C-lobe is not completely understood but could arise from crystal-packing effects (Anderson *et al.*, 1990).

Here a detailed analysis is presented of the structural mechanism underlying the movement of N1 and N2. The atomic co-ordinates of the closed form are taken from the protein data bank (Bernstein *et al.*, 1977), identifier 1LFG. Co-ordinates for the open form are from a further refinement of the previously deposited co-ordinates (1LFH). These structures were determined at resolutions of 2·2 Å and 2·0 Å with crystallographic *R*-factors of 0·178 and 0·176, respectively.

In addition to the domain closure in the N-lobe, superpositions (Baker *et al.*, 1991) have shown that in the iron-free form of lactoferrin, there is a small (8°) rotation of the C-lobe relative to the N-lobe. This rotation is about an axis perpendicular to the N1–N2 rotation axis (which is discussed below), and there is no direct contact between N2 and the C-lobe. Thus, any coupling between the motion of N2 and the motion of the C-lobe is indirect and will not affect the discussion presented below of the domain closure in the N-lobe.

Table 1
Regions in lactoferrin

Name	Residues[a]	R.M.S.[b]
N-lobe	1–344	
C-lobe	345–691	
N1	1–91, 252–333	
N2	92–251	
N1 core[c]	5–84, 252–301, 304–331	0·45
N2 core[c]	92–100, 104–138, 144–218, 221–250	0·39
Helix 5	121–136	
Helix 11	321–332	

[a]The definitions of the lobes, domains, and secondary structures are taken from Anderson *et al.* (1989).

[b]R.M.S. deviation (in Å) of the main-chain atom positions after fitting either the N1 or N2 core region of the open and closed forms.

[c]The static cores of the N1 and N2 domains were identified by a sieve-fit procedure (Lesk, 1991). A 0·4 Å threshold was used. This value is approximately the same as the expected experimental error in the co-ordinates. Most of the residues excluded from the static core (101 to 103, 139 to 143, and 219 to 220) are part of flexible loops, and differences in their conformation are unlikely to be linked to the overall motion. In contrast, the peptide flip at 302 to 303 lies at the domain interface and is more closely coupled to the closure motion.

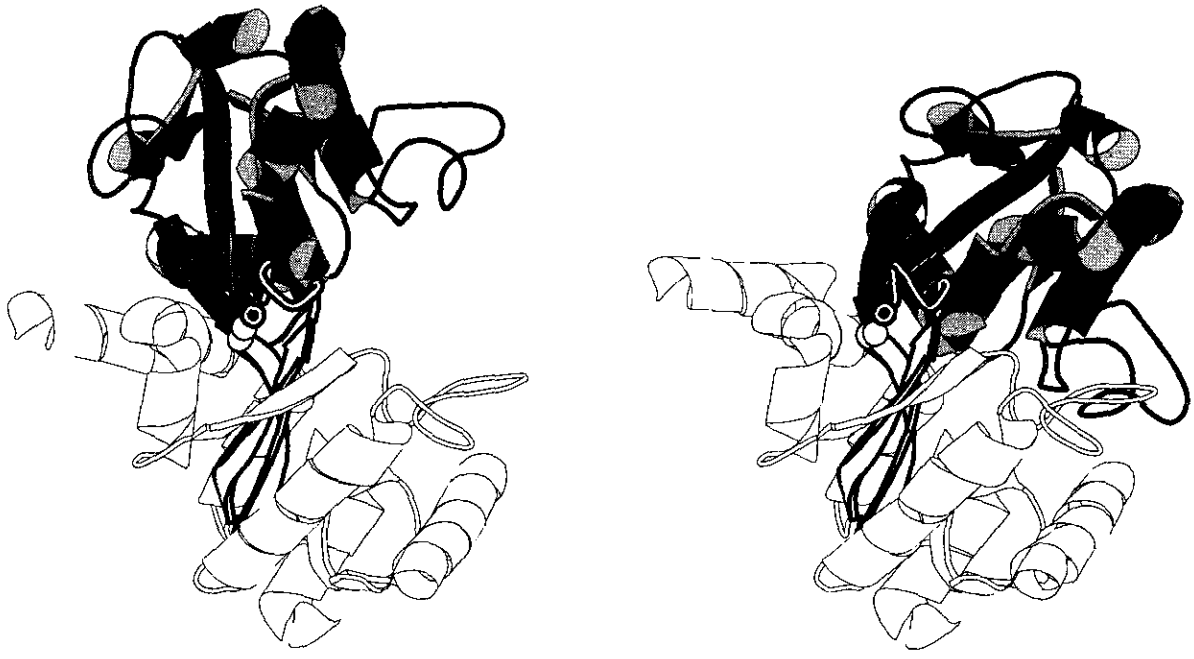

Figure 1. The overall motion in lactoferrin. The Figure shows N1 and N2 of lactoferrin in open (a) and closed (b) forms, with the N1 cores (Table 1) of both forms superposed. The origin of the screw transformation lies at the center of the Figure, and the view is down the screw axis, which is indicated by a circle with a dot in it. N2 is shown in darker shading than N1, and the antiparallel β-strands that contain the two hinges are highlighted with a bold line. The C^{α} atoms of residues 90 and 251, which lie in the middle of these strands, lie very near the screw axis in the open form and are indicated by open circles. This Figure as well as Figs 2 and 4 were produced with MOLSCRIPT (Kraulis, 1991). To assess how close the direction of the screw axis is to the line through the C^{α} atoms of residues Thr90 and Pro251, the total 54° rotation $\mathbf{R}_0$ can be decomposed into a rotation $\mathbf{R}_1$ around an axis connecting C^{α} atoms of Thr90 and Pro251 followed by a rotation $\mathbf{R}_2$ around an axis perpendicular to that of $\mathbf{R}_1$. A similar decomposition can be done using the axis of helix 11 and is shown in the table below. (l, m, and n refer to the 3 direction cosines of a rotation axis, and κ refers to the rotation angle around that axis.)

	$\mathbf{R}_0$	=	$\mathbf{R}_2$	$\mathbf{R}_1$	=	$\mathbf{R}_{2'}$	$\mathbf{R}_{1'}$
	Total rotation of N2 relative to N1		Rotation around axis perpendicular to that of $\mathbf{R}_1$	Rotation around axis connecting C^{α} atoms of 90 and 251		Rotation around axis perpendicular to that of $\mathbf{R}_{1'}$	Rotation around axis of helix 11
l	0		0·049	0·074		−0·78	0·42
m	0		−0·99	−0·16		−0·50	0·043
n	1		0·16	0·98		0·38	0·91
κ	54·1°		9·4°	53·4°		22·0°	49·8°

3. Overall Description of the Motion

(a) *The static core and the principal movers*

As discussed in the legend to Table 1, a sieve-fitting procedure was used to identify a set of residues, called the static core, in each domain that did not move appreciably with respect to each other. The residues forming the static cores of N1 and N2 are listed in Table 1. They do not include the regions linking the domains, some residues in the interface between N1 and N2, and some surface loops far from the interface. On the whole, however, the static cores include most of the residues in the protein, 90% of N1 and 93% of N2. This result provides further evidence that N1 and N2 move as rigid bodies (Baker *et al.*, 1991). After superposing on the static core of N1, the maximum C^{α} displacement of any residue in the N2 core is 27 Å.

(b) *The rigid-body rotation of N2 relative to N1 around a screw axis*

To characterize the rigid-body motion of N2 relative to N1, the open and closed forms were superposed on the static core of N1. Then the further rotation and translation required to superpose them onto the N2 core were determined. The rotation is 54°. The magnitude and direction of the translation depend upon the choice of origin for the rotation axis.

Describing the motion as a screw motion fixes the origin so that the translation is minimal and occurs

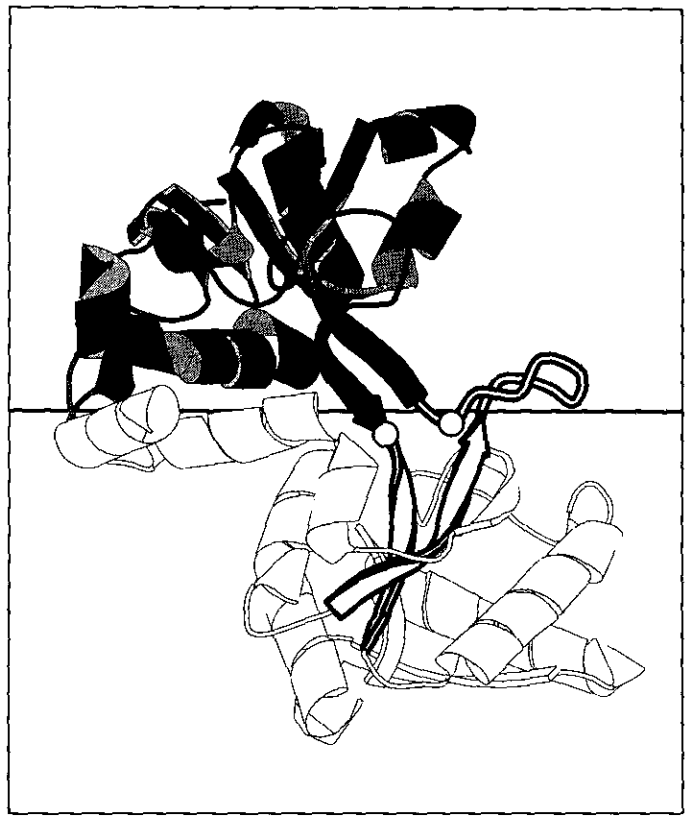

(a)

Fig. 2.

along the rotation axis (see Appendix). With such a choice of origin, N2 translates only 1·0 Å, and as is evident in Figure 1, the screw axis passes very close to Thr90 and Pro251, the two residues previously identified to be at center of the hinges (Anderson *et al.*, 1990). In particular, the screw axis passes within 1·4 Å of the C^{α} of Thr90 and within 2·4 Å of the C^{α} of Pro251 and is nearly parallel to a line through these two C^{α} atoms. As discussed in the legend to Figure 1 and in the Appendix, the 54° rotation about the screw axis can be decomposed into a 53° rotation about this line followed by a 9° rotation about an axis perpendicular to it. Thus, when described as a "screw motion," the motion of N2 relative to N1 is almost a pure rotation about the central residues in each hinge.

(c) *Torsion angle changes in the hinge region*

The main-chain around the hinges has the form of two antiparallel β-strands with an inserted loop (Figs 1 and 2). The principal torsion angle changes involved in the hinge motion are in $\psi(90)$, $\phi(91)$, $\phi(250)$, $\psi(250)$, and $\phi(251)$. With the current coordinates, these are the largest changes in the hinge region and are, respectively, 49°, 26°, 30°, 33°, and 22° (Table 2).

In a pure hinge motion, the axes of the principal torsion angle changes would be parallel to the axis of the overall rotation. The angles between the screw axis and the axis of each torsion angle rotation are shown in Table 2. Clearly, the axes of rotation for $\Delta\psi(90)$, $\Delta\phi(91)$, $\Delta\psi(250)$, and, to a lesser extent, $\Delta\phi(251)$ are better aligned with the screw axis than the axes for the other torsion angle changes in the hinge region. So the principal torsion angle changes have rotation axes in roughly the same direction as the overall rotation.

The first hinge involves torsion angle changes in $\psi(90)$ and $\phi(91)$. These changes are coupled across a peptide bond, and as they are in the same direction, they do not cancel. They produce a total rotation of 81° around a virtual bond connecting the C^{α} atoms of Thr90 and His91, i.e., in the pseudo torsion angle α. The axis of this α-angle rotation is inclined only 34° relative to the screw axis, and this inclination is consistent with the axes of $\Delta\psi(90)$ and $\Delta\phi(91)$ being in same direction as the overall motion. The magnitude of the α-angle rotation is greater than the overall 54° rotation, so the changes in $\psi(90)$ and $\phi(91)$ essentially rotate N2 in the correct direction, but by $\sim 30°$ too much. Small changes in neighboring torsions compensate for this excess. Because of this cancellation, a rotation of just $\psi(90)$ alone is able to reproduce much of the motion of the first hinge.

In the second hinge the principal torsion angle changes do not have their rotation axes as closely aligned with the screw axis as do $\Delta\psi(90)$ and $\Delta\phi(91)$, and the description of this hinge is not as simple. Three torsion angles have changes greater than 20°: $\phi(250)$, $\psi(250)$, and $\phi(251)$. The change in the central torsion angle, i.e. $\Delta\psi(250) = -33°$, is the

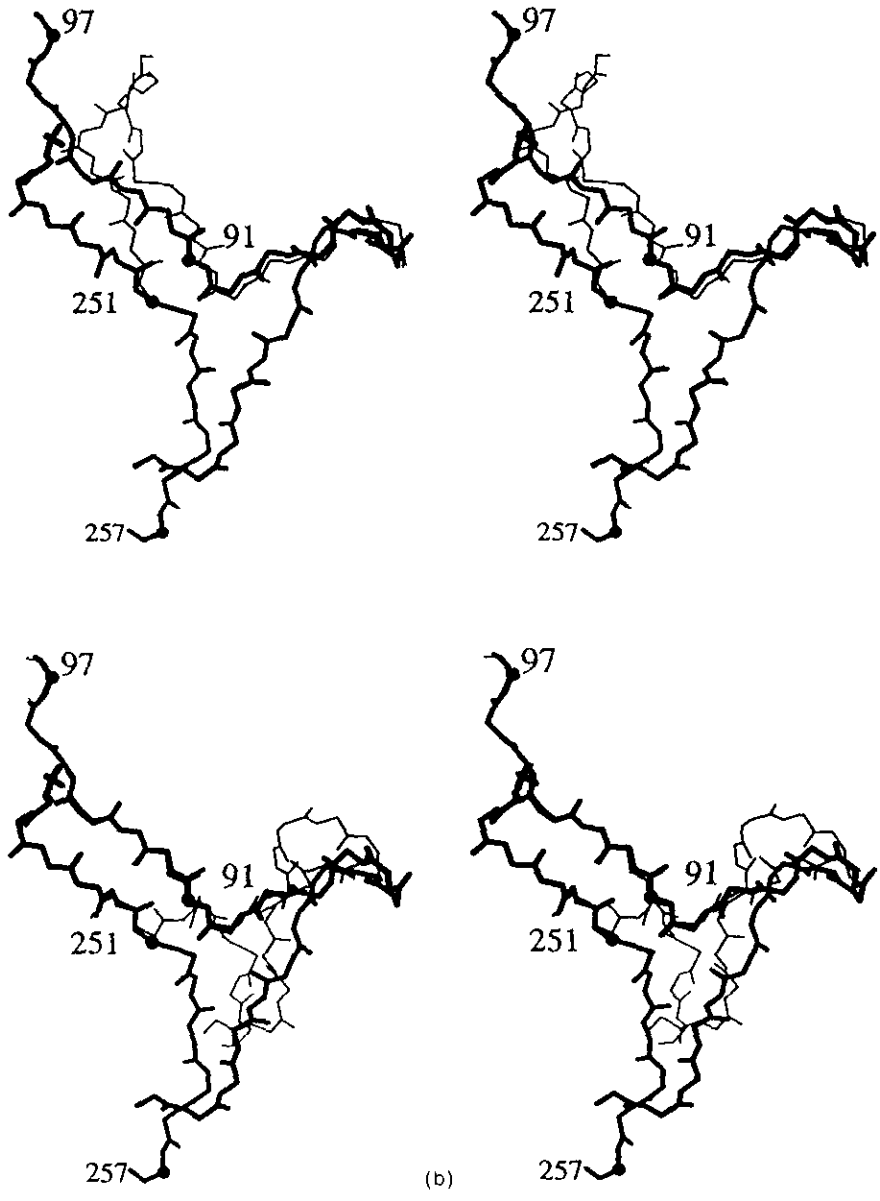

Figure 2. The two hinges in lactoferrin. (a) The open form as shown in Fig. 1(a) but rotated by 90°, so the screw axis, indicated by a thick line, is parallel to the plane of the page and perpendicular to the viewing direction. (b) A close up of the hinges in stereo. The view is approximately the same as that in (a) but only the main-chain atoms of the hinge region are shown. The main-chain atoms of the closed form are shown by the thick line, and those of the open form, by thin line. The open form is fit onto the closed form using residues in N1 (top) and in N2 (bottom). The principal residues of the hinges are Thr90 and His91 and Val250 and Pro251.

largest of the three and has an axis most closely aligned with the screw axis (considering both forms). This change is coupled across the peptide bond with $\Delta\phi(251)$ to produce an α-angle rotation of 49°. However, as the axes of $\phi(251)$ and $\psi(250)$ are not as closely aligned with the screw axis as those of $\psi(90)$ and $\phi(91)$, this 49° α-angle change is less closely aligned with the overall motion than the 81° α-angle rotation in the first hinge. A rotation in a direction perpendicular to the screw axis is necessary and is supplied by $\phi(250)$.

In sum, the analysis suggests that $\psi(90)$ in the first hinge and $\phi(250)$ and $\psi(250)$ in the second hinge are the three most important torsion angles in the lactoferrin domain closure. Flipping these three angles from their open to closed conformation replicates roughly 75% of the total motion. That is, N2 in open form with these three torsions changed is rotated 41° with respect to the open form N2 and −14° with respect to the closed form N2 with both rotations roughly in the same direction as the overall 54° rotation (the rotation axes are inclined 8° and 23° to the screw axis).

$\phi(91)$ and $\phi(251)$ are of lesser importance than $\psi(90)$, $\phi(250)$, and $\psi(250)$. Furthermore, there are a number of other appreciable (greater than 10°) main-chain torsion angle changes in the hinge region: five between 249 and 252 and 13 between 84 and 91. These changes contribute the remainder of the motion. Many of them can be grouped into

Table 2
Torsion angle changes in the hinges

Residue	Torsion angle change[a]	Angle with screw axis[b] Open	Closed	Residue	Torsion angle change[a]	Angle with screw axis[b] Open	Closed
A. *Changes in ϕ and ψ*							
ψ	4			ϕ 248	7	−75	−80
84 ϕ	−15			ψ	−8	−21	−24
ψ	−15			ϕ 249	16	−25	−23
85 ϕ	−1			ψ	−6	82	79
ψ	147			ϕ* 250	**30**	**84**	75
86 ϕ	−168			ψ*	**−33**	**−26**	−41
ψ	17			ϕ* 251	**−22**	**−35**	−50
87 ϕ	−3	30	34	ψ	14	−81	−81
ψ	−36	41	44	ϕ 252	0	−71	−71
88 ϕ	12	48	47	ψ	9	65	65
ψ	−20	28	41				
89 ϕ	22	20	35				
ψ	−16	59	53				
90 ϕ	−2	56	51				
ψ*	**−49**	**14**	23				
91 ϕ*	**−26**	**16**	25				
ψ	15	89	89				
92 ϕ	4	78	86				
ψ	−4	38	38				

[a]The 5 torsion angles that are highlighted by a star (*) and are shown in **bold** are the principal contributors to the overall domain closure motion. Changes in ψ_i and ϕ_{i+1}, the torsion angles on either side of the peptide bond, can be coupled. If $\Delta\psi_i \approx -\Delta\phi_{i+1}$ and both are small in magnitude, they approximately cancel. That is, while the peptide orientation changes considerably, the chain direction does not. Cancelling pairs of $\Delta\psi_i$ and $\Delta\phi_{i+1}$ are boxed in the Table.

The cancellation of torsion angles was verified by an exhaustive conformational search using CHARMM and X-PLOR (Brooks *et al.*, 1983; Brünger *et al.*, 1987). All possible combinations of torsion angles in the hinge region were changed from their values in the open form to those in the closed form. The new changed structure was fit onto the N1 core of lactoferrin and the r.m.s. deviation for atoms in the N2 core was calculated. The r.m.s. deviation was then used to rank the various torsion angle changes. In particular, the conformational search shows that just changing $\psi(90)$ reproduces remarkably well the effect of all 13 torsion angle changes in the first hinge.

Residues 84 to 89, which form a β-hairpin that extends out from the structure, were difficult to fit into the electron density. Consequently, the torsion angle changes in this region may not be as certain as in other parts of the structure. In any case, as is evident from the Table and the conformational search, the changes in the region effectively cancel out.

[b]The last 2 columns show the angle between the screw axis and the axis of the torsion rotation (i.e. the line connecting either the N and C^{α} atoms or C^{α} and C atoms) for both the open and closed forms. Clearly, the principal torsion angle rotations are in the same direction as the overall motion.

	Between residues	Δα	Angle with screw axis	Between residues	Δα	Angle with screw axis
B. *Changes in α*						
	84–85	−12		247–248	0	
	85–86	24		248–249	3	24
	86–87	−31		249–250	−15	88
	87–88	10	59	250–251*	**49**	**47**
	88–89	−11	7	251–252	−5	59
	89–90	38	54	252–253	−9	72
	90–91*	**81**	**34**			
	91–92	−33	65			
	92–93	0	45			

Changes in α angles for the residues in the hinge. α angles are torsion angles for rotations around the virtual bonds connecting C^{α} atoms. Major α angle changes are highlighted by stars (*). The angles between the screw axis and the axes of each α-angle rotation are also shown. The α-angle axes are lines connecting the C^{α} atoms in the open form.

canceling pairs of rotations on either side of the peptide bond (as is discussed in Table 2).

As shown in Figure 3, all the principal torsion angle changes in lactoferrin occur in normally allowed regions of the Ramachandran diagram and consequently involve only low-energy transitions.

4. Changes in the Large and Small Interfaces

(a) *Accessibility and packing of the interfaces*

Excluding the residues in the hinges, the 39 residues making contacts between N1 and N2 can be grouped into two domain interfaces on either side of

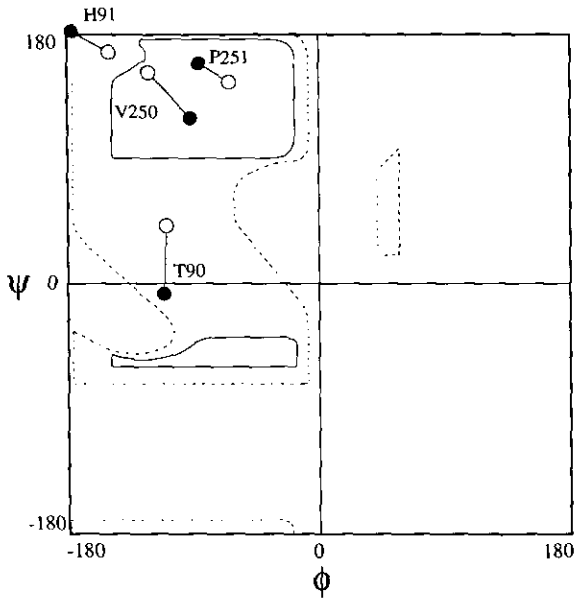

Figure 3. Ramachandran diagram of the main torsion angle changes in lactoferrin. $\phi\psi$-values of the 4 residues in the hinges are shown with open circles for the open conformation and with filled circles for the closed conformation. The open and closed $\phi\psi$-values of the 4 residues are:

Thr90 $(-110°, 42°) \rightarrow (-111°, -7°)$,
His91 $(-150°, 167°) \rightarrow (-176°, -178°)$,
Val250 $(-122°, 153°) \rightarrow (-92°, 119°)$,
Pro251 $(-64°, 146°) \rightarrow (-86°, 159°)$.

All the transitions are in normally allowed regions of the diagram. Note that proline has a more restricted range of allowed $\phi\psi$-values. In addition to being in an allowed region of the normal Ramachandran diagram, its ϕ value is usually constrained to be between $-100°$ and $-40°$ (Creighton, 1984; Kolaskar & Kulkarni-Kale, 1992).

the screw axis. Here these interfaces are called the large and small interfaces. In the open form, the small interface is buried and close-packed while residues in the large interface are accessible to solvent. The situation is reversed in the closed form: residues in the small interface become exposed to solvent, and those in the large interface become buried and pack closely. As listed in Table 3, the large interface contains 26 residues, which primarily line the two walls of the interdomain binding cleft. The small interface contains 13 residues. It is made from residues packed between helices 5 and 11, which are associated with N2 and N1, respectively.

The alternate exposing and burying of the interfaces on either side of the screw axis resembles the motion of a see-saw. This alternation is evident in the sections through the van der Waals envelope of lactoferrin shown in Figure 5. It is also evident in terms of the solvent accessibility (Lee & Richards, 1971) and volumes of the interface residues (Richards, 1974; Chothia, 1975). Upon closure, the accessible surface area decreases for each residue in the large interface and increases for each residue in the small interface. These increases and decreases are neatly arranged on either side of the screw axis (Fig. 4(a)). In total, upon closure ~ 900 Å^2 of accessible surface is buried in the large interface while ~ 300 Å^2 becomes accessible in the small interface, giving a total increase of ~ 600 Å^2 of buried surface area between the two interfaces.

Upon closure 16 of the 26 large interface residues are buried and close-packed. That is, they have an accessible surface of less than 20 Å^2 and residue volumes close to those normally found in the protein core (Chothia, 1984). Conversely, nine of the small interface residues close pack only in the open form. (Two residues are close-packed in both forms.) As was the case with accessibility, the changes in packing are neatly arranged around the screw axis (Fig. 4(b)).

The close packing of the interfaces is achieved with only moderate changes in the conformation of side-chains. Of the 33 interface side-chains with a χ_1 torsion angle, only six have large changes (more than 35°), and of the 29 side-chains with a χ_2 only eight have large changes. Many of the side-chains that change conformation are involved in specific interactions. Asp60 is an iron ligand and Arg210 is also associated with the iron-binding site. Lys296 and Lys301 form interdomain salt bridges upon domain closure. Tyr324, Arg133, and Arg332 (respectively, at N terminus of helix 11, C terminus of helix 5, and C terminus of helix 11) change conformation to accommodate the relative movements of helix 5 and helix 11. For the remaining interface side-chains, $\langle\Delta\chi_1\rangle$ and $\langle\Delta\chi_2\rangle$ are just 10° and 15°, respectively. The implication is that most of the side-chains just rock slightly in a local potential well and that only about a quarter of the side-chains change to a different rotamer conformation (Ponder & Richards, 1987). In total, the conformational changes in the interface side-chains are responsible for ~ 100 Å^2 of the ~ 600 Å^2 of buried surface.† Thus, when open, the interfaces are largely preformed to fit together tightly when closed.

(b) *Packing of helix 5 and helix 11*

The interface between helix 5 and helix 11 (the 5–11 interface) has been divided between the large and small interfaces. Helix 5 and helix 11 are packed in a crossed fashion (interhelical angle 62°), and helix 5 moves with N2 while helix 11 remains fixed with N1. As evident in Figure 1, the axis of

† *The accessible surface area can be calculated* separately for the domain–domain contact residues in N1 and N2 in both the open and closed forms to give 4 quantities: A(N1,O), A(N1,C), A(N2,O), and A(N2,C). By separately, one means that in calculating A(N1,O) none of the atoms in N2 are considered. The change in surface area brought about purely by the *conformational changes in interface side-chains is:*

$A(N1,O)+A(N2,O)-A(N1,C)-A(N2,C) \approx 100$ Å^2.

Note, this value excludes all burial of surface due to the relative motion of N1 and N2.

Table 3
Residues in the large and small interfaces and in the hinges

	N1–N2 contact[a]					Area[c]			Volume[d]			
	O	C	SS[b]	Residue		O	C	C–O	O	C	$\Delta\chi_1$	$\Delta\chi_2$
Large	—	√	2	**42**	Pro	35	16	−19	—	130	7	7
interface	—	√	3	**60**	Asp	58	10	−48	—	122	(83)	(75)
N1	—	√	3	**61**	Gly	20	0	−8	—	66	—	—
	—	√	3	**62**	Gly	36	2	−34	—	62	—	—
	—	√	3	**63**	Phe	66	14	−52	—	249	12	33
	—	√	3	**66**	Glu	50	24	−26	—	—	6	7
	—	√	d	**82**	Tyr	40	10	−30	—	210	6	22
	—	√	j	**253**	His	49	19	−30	—	173	5	1
	—	√	—	**296**	Lys	154	101	−53	—	—	(59)	(171)
	—	√	—	**301**	Lys	67	10	−57	—	164	22	(51)
	—	√	11	**328**	Ile	27	3	−24	—	171	0	29
	√	√	11	**331**	Leu	40	11	−29	—	196	9	7
	√	—	11	**332**	Arg	128	100	−28	—	—	(39)	6
Large	—	√	—	**120**	Arg	147	93	−54	—	—	31	(74)
interface	—	√	5	**121**	Arg	54	20	−34	—	—	14	3
N2	√	√	5	**122**	Thr	38	0	−38	—	130	3	—
	√	√	5	**126**	Asn	44	11	−33	—	127	9	9
	√	—	5	**129**	Ile	0	0	0	181	165	3	34
	√	√	—	**141**	Pro	72	68	−4	—	—	3	0
	√	—	6	**145**	Ile	27	13	−14	—	170	13	(101)
	—	√	—	**183**	Phe	102	43	−59	—	—	1	12
	—	√	7	**192**	Tyr	49	6	−43	—	188	2	2
	—	√	7	**193**	Ser	60	22	−38	—	—	(62)	—
	—	√	h	**210**	Arg	52	3	−49	—	179	(53)	27
	—	√	8	**216**	Glu	131	67	−64	—	—	23	5
	—	√	8	**217**	Asp	53	38	−15	—	—	11	31
Sum/Avg[g]						1599	704	−895		2502	9	14
Small	√	—	11	**323**	Gly	27	55	28	—	—	—	—
interface	√	√	11	**324**	Tyr	14	25	11	204	—	10	(57)
N1	√	—	11	**327**	Ala	1	48	47	89	—	—	—
	√	√	11	**330**	Asn	18	29	11	134	—	0	14
	√	√	—	**333**	Lys	43	63	20	—	—	(42)	22
Small	√	√	5	**127**	Val	0	13	13	128	136	2	—
interface	√	√	5	**130**	Gly	0	35	35	63	—	—	—
N2	√	—	5	**131**	Thr	36	50	14	—	—	14	—
	√	√	5	**133**	Arg	5	30	25	211	—	14	(60)
	—	—	5	**134**	Pro	42	82	40	—	—	24	32
	√	√	—	**138**	Trp	8	25	17	229	—	13	4
	√	—	j	**247**	Leu	9	24	15	164	—	15	(37)
	√	—	j	**248**	Ala	1	32	31	87	—	—	—
Sum/Avg[g]						204	511	307	1309		12	18
Hinge 1			—	**89**	Arg	77	49	−28	—	—	(96)	17
			—	**90**	Thr	24	42	18	—	—	(50)	—
			e	**91**	His	24	27	3	—	—	3	(41)
			e	**92**	Tyr	30	0	−30	—	185	11	18
Hinge 2			j	**249**	Arg	28	133	105	—	—	26	(61)
			j	**250**	Val	10	2	−8	126	127	(75)	—
			j	**251**	Pro	14	21	7	133	—	8	11
			j	**252**	Ser	4	0	−4	93	94	16	—
Environ-			d	**79**	Ala	1	0	−1	91	88	—	—
ment			d	**80**	Glu	2	1	−1	155	150	29	28
of the			d	**81**	Val	18	15	−3	145	140	2	—
hinge[f]			—	**87**	Gln	118	139	21	—	—	(124)	(95)
			e	**93**	Tyr	9	5	−4	195	220	12	7
			e	**94**	Ala	1	1	0	91	88	—	—
			j	**254**	Ala	1	0	−1	95	91	—	—
			k	**308**	Ser	27	29	2	—	—	(37)	—
			10	**319**	Tyr	3	10	7	203	198	5	10
			10	**320**	Leu	0	7	7	160	165	8	6
Sum/Avg[g]						391	481	90	1671	1546	12	14

Table 3 *continued*

[a]Each interface residue makes at least one contact between the domains. Contacts were defined as atoms separated by less than the sum of their van der Waals radii plus 0·6 Å and found using programs written by A. M. Lesk. Whether the contact occurs in the open (O) or closed (C) form is indicated in the Table.

[b]Column SS refers to the secondary structure that a given residue has.

[c]*Accessible surface area (Lee & Richards, 1971) in the open and closed form was calculated with the program* ACCESS (M. Handschumacher & F. M. Richards, 1983). *The calculations were done on the* N and C *lobe together. They did include the iron and the* CO_3^{2-} *ion but excluded crystallographic "bound" waters and a weakly bound, poorly defined* EDTA *molecule.*

[d]Residue volume in the open and closed form was calculated using the program VOLUME (Richards, 1979). Rather than the original Voronoi procedure, in which a plane bisects the interatomic vector, Richards' method B was used. Method B uses the ratio of the van der Waals or covalent radii of neighboring atoms to proportion the interatomic vector. Radii for both surface and volume calculations were taken from Chothia (1975). The volume calculations were done on the whole molecule, N and C lobe together. They *included* all crystallographic bound waters, the irons, and all other ligands. Volumes for residues that have accessible surface area of 20 $Å^2$ or more are not shown.

[e]Also listed is the change (between open and closed form) in the first 2 side-chain torsion angles. Movements more than 35° are indicated by parentheses.

[f]*The environment of the hinge is defined as the residues that are not in either the large interface, the small interface, or the 2 hinge regions, but that make contact with the hinge residues.*

[g]*This row shows the total area and volume for each grouping, the large and small interfaces and the hinge and its environment. It also shows the average of all torsion angle changes less than 35°, i.e. the average of those changes not enclosed by parentheses. For comparison, the standard residue volumes listed by Chothia (1984) can be used to compute the volumes of the interfaces. Doing this calculation for the large interface in the closed form and the small interface in the open form, one finds the total volumes are 2525 $Å^3$ and 1339 $Å^3$, respectively. These volumes agree with total volumes listed in the Table (to within 3%), and this agreement provides further indication that the interfaces are close packed.*

helix 11 is roughly parallel to the screw axis. Consequently, upon closure helix 5 rotates ~50° around helix 11 (see the legend to Fig. 1). However, since the helix 11 axis is displaced from the origin of the screw axis, helix 11 and helix 5 translate and move apart by 2 Å (as measured from the distance between helix axes). As shown in Figure 5(a), this motion exposes one part of the 5–11 interface. In particular, two small side-chains (Ala327 and Gly130) at the center of the interface pack closely in the open form. However, in the closed form they lose contact, and a cavity, filled by three water molecules, is formed between them. The residues immediately surrounding Gly130 and Ala327 are large and retain contacts in both forms.

The motion of helix 5 relative to helix 11 buries

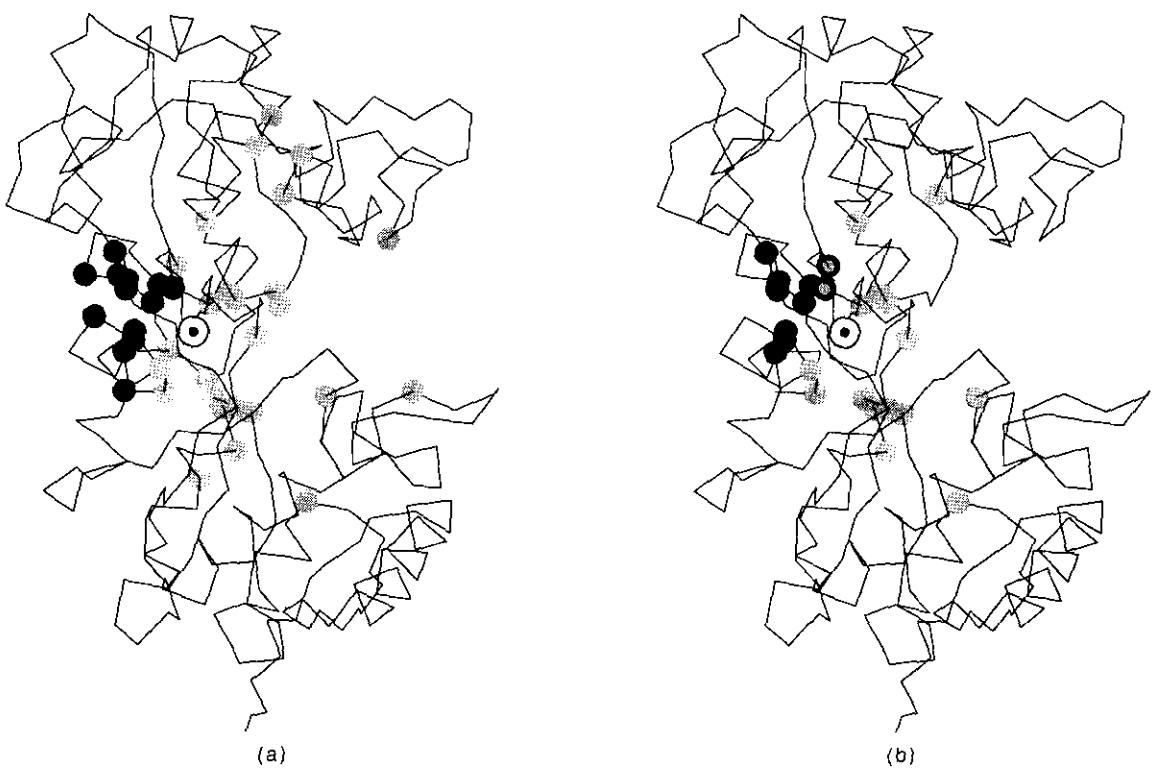

Figure 4. The large and small interfaces in lactoferrin. The view for both parts of the Figure is down the screw axis as in Fig. 1, and the screw axis is indicated by a circle with a dot in it. (a) Differences in accessible surface area of the residues in the large and small interface. Dark circles show the residues more exposed in the closed form, and lightly shaded circles show the residues more buried. (b) Change in packing of the residues in the large and small interfaces. Dark circles show residues that close pack in the open form only; lightly shaded circles show residues that close pack in the closed form only; and lightly shaded circles with a dark border show residues that close pack in both forms.

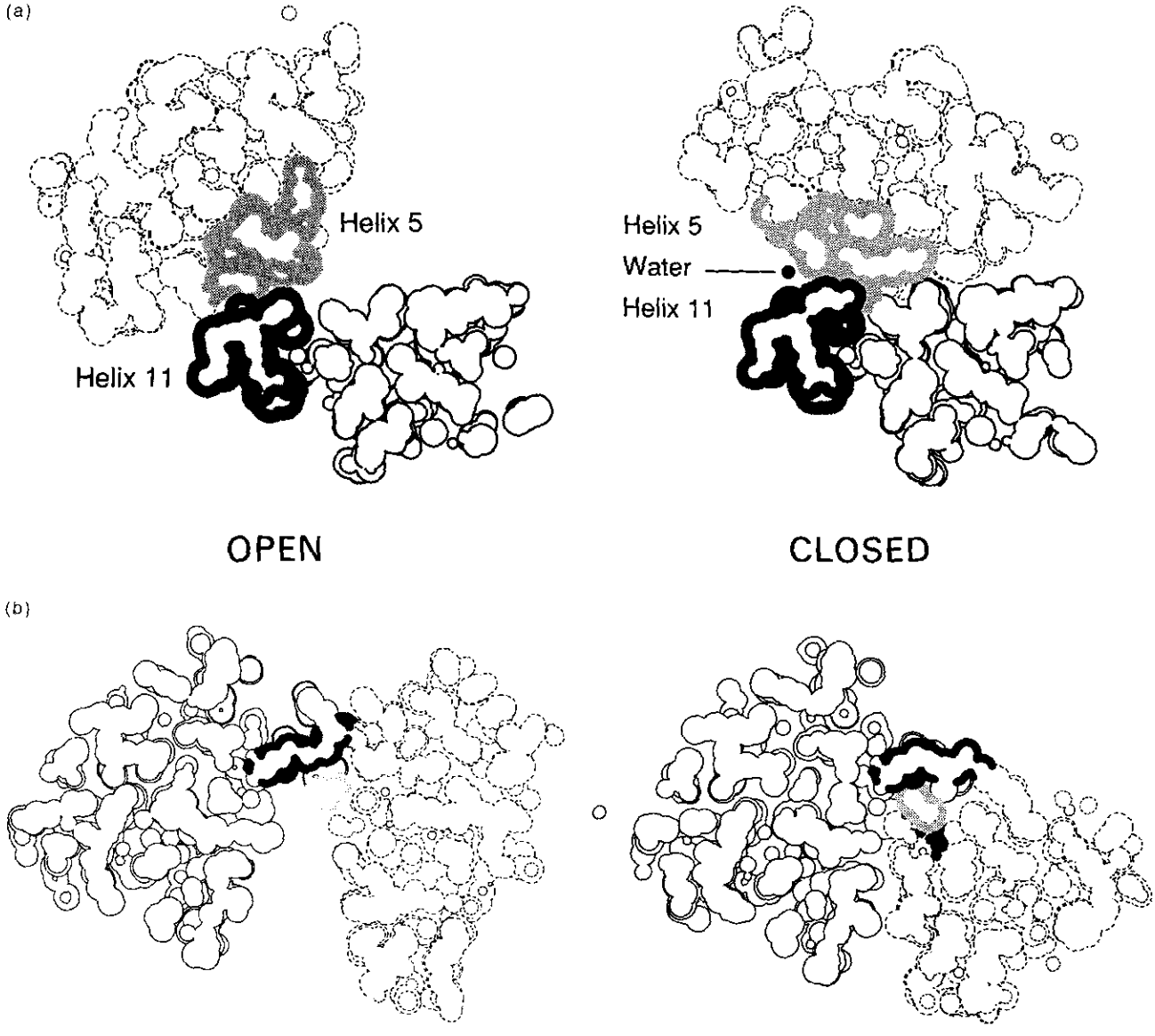

Figure 5. Slices through the van der Waals envelope of lactoferrin. In both parts of the Figure, the open form is shown at left and the closed form at right, and N1 is represented by a thin black line, and N2, by a dotted black line. In (a, top), the molecule is orientated so the viewer is looking down the screw axis, as in Fig. 1. However, in (b, bottom) the molecule is tipped slightly so the viewer is looking down the cleft. In this "cleft" view, the 2 domains appear most separate, and the screw axis is inclined ~ 35° to the page normal. (a, top) The small interface. Helix 5 is shown in light gray and helix 11 in dark gray. When these 2 helices separate in the closed form, 3 water molecules (the 38th, 39th, and 40th waters in the Brookhaven file) fill the gap. One of these water molecules (39) is indicated. (b, bottom) The large interface. The main-chain atoms of the hinge (89 to 92 and 249 to 252) are shown in bold black line, and the side-chain of Tyr92, in light gray line. The iron is shown in dark gray.

another part of the 5–11 interface. This is evident in the decrease in accessibility and increase in close packing of a number of residues listed in Table 3 (Arg121, Thr122, Asn126, Ile129, Pro141, Ile145, Ile328, Leu331, and Lys332). To maintain their packing three of these residues change conformation (Lys332, Ile145, and, to a lesser extent, Ile328). The alternate exposing and burying of parts of the 5–11 interface strongly contrasts with the motion of packed helices involved in shear motions as in citrate synthase or in insulin. In shear motions helices retain the same close-packed configuration, and this close-packing, in turn, constrains main-chain motions to be less than ~2 Å (Chothia *et al.*, 1983).

5. Environment of the Hinges

(a) *Sides facing the large and small interfaces*

The two hinges lie on the screw axis and so face toward both the large and small interfaces. Consequently, upon closure the side of the hinges that faces towards the large interface becomes more

Table 4
Transferrin sequences in the hinge regions

Species[a]		88	89	90	91	92	93	244	249	250	251	252	253
Human	Lactoferrin	P	R	T	H	Y	Y	A	R	V	P	S	H
Mouse	Lactoferrin	P	R	T	H	Y	Y	A	Q	V	P	S	H
Cow	Lactoferrin	P	Q	T	H	Y	Y	A	Q	V	P	S	H
Pig	Lactoferrin	P	Q	T	Y	Y	Y	A	R	V	P	S	H
Human	Transferrin	P	Q	T	F	Y	Y	A	E	V	P	S	H
Rabbit	Transferrin	P	K	T	F	Y	Y	A	R	V	P	S	H
Pig	Transferrin	P	Q	T	H	Y	Y	A	Q	V	P	S	H
Horse	Transferrin	P	Q	T	H	Y	Y	A	S	I	P	S	H
Frog[b]	Transferrin	T	D	T	C	Y	Y	A	K	V	P	A	H
Chicken	Ovotransferrin	S	T	T	S	Y	Y	A	R	V	A	A	H
Human	Melanotransferrin	V	G	T	S	Y	Y	A	R	V	P	A	H
Hornworm[c]	Transferrin	A	P	F	R	Y	E	A	A	R	P	W	Q

[a]Sequence numbering is for the human lactoferrin, the sequence and structure discussed here. Sequences are from the sequence databanks, PIR and SwissProt.
[b]*Xenopus laevis*.
[c]*Manduca sexta*.

buried while the side that faces toward the small interface becomes more exposed (Table 3). The burying of the large-interface side is most interesting. In a pure hinge motion the packing at the base of the hinge is crucial. There is little space for accommodation, and the two interfaces must fit together perfectly to avoid steric clashes. Furthermore, in a true hinge the deformation takes place over only a few main-chain torsion angles, so there is little freedom for slight adjustments to improve the fit of the interfaces. Such characteristics of an ideal hinge are found in lactoferrin. In the closed form, the atoms of the hinge pack closely with the large interface and with the iron and the CO_3^{2-} ion. Tyr92, in particular, is slightly exposed in the open form, as shown in Figure 5(b). However, in the closed form it is able to fit snugly at the very base of the hinge without large changes in its side-chain torsions. As one of the four iron ligands, it is completely buried.

There is a large water-filled cavity near the iron in the closed form (Anderson *et al.*, 1989). It does not appear to affect the hinge directly but it perhaps facilitates the overall packing of the large interface.

(b) *Main-chain of the hinges*

In most sections of a protein the main-chain is deeply buried beneath layers of side-chains. There is little freedom for large torsion angle changes. Such steric constraints necessitate that many protein movements proceed by shear mechanisms, which involve small torsion angle changes distributed over many residues. In lactoferrin, the main-chain atoms of the hinge are remarkably free from steric constraints. In fact, in the open form, the main-chain atoms of Thr90, His91, and Pro251 make no contacts with the rest of the protein; the main-chain atoms of Arg249 make only one contact; and the main-chain atoms of Tyr92 and Val250 make only three contacts per residue. (Contacts are calculated between the two hinge regions *taken as a whole*, 89 to 92 and 249 to 252, and the rest of the protein, 1 to 88, 93 to 248, and 253 to 691.) This unusual packing is clearly visible in Figure 5(b) and is present only in the open form. Given only the open form, it seems possible to identify the hinges.

There are, however, additional contacts involving main-chain atoms *within* the hinge region. In particular, there are four hydrogen bonds "internal" to the hinges (252 N···O 90, 89 NH1···O 91, 250 N···O 92, 92 N···O 250). These are maintained in both open and closed forms and may help co-ordinate the motion of the two hinges.

The absence of main-chain packing constraints with the rest of the protein, coupled with many "internal" hydrogen bonds, was also found in the hinged mechanisms in lactate dehydrogenase (Gerstein & Chothia, 1991) and in adenylate kinase (Gerstein *et al.*, 1993) and appears to be a crucial structural requirement for hinged motion.

(c) *Sequence conservation in the hinges*

The sequences of at least 12 transferrins have been published, and in Table 4 they are compared around the two hinges. Except for the hornworm sequence, which is very different, the 12 sequences are very similar around the hinges. The metal ligands, Tyr92 and His253, are, of course, conserved for functional reasons. Close-packing in at least one form (open or closed) explains why Tyr93, Ala248, Val250, and Pro251 are conserved. This close-packing and conservation is also true, to a lesser extent, for Pro88 and Ser252. Conversely, the exposure and absence of closepacking in both forms explains why Arg89 and Arg249 are not conserved. The low sequence conservation of these two side-chains, in turn, suggests that their motion is a consequence rather than a cause of the domain

closure. As Thr90 is exposed, its conservation is hard to explain. Two proline residues are present in most of the transferrin sequences. Prolines are also present in the hinge regions of several bacterial binding proteins (Mowbray, 1992) and could perhaps modulate the motion at the hinge.

6. Dynamic Implications of the Hinge Motion

The dynamics of the lactoferrin domain movement depend on how easily the hinge motion can assemble the interfaces and, in particular, the iron-binding site; the different interactions at the interfaces in the open and closed forms; and the energetic details of the conformational change in the hinge region itself.

The conformational change in lactoferrin requires that some of the groups that bind the iron be located on one domain and some on the other. One iron-binding group (Asp60) is on the N1 domain, three (Tyr192 and two oxygens from a bound CO_3^{2-} ion) are on the N2 domain, and the remaining two (Tyr92 and His253) are on the two interdomain strands containing the hinges. The location of the hinges with respect to the last two groups is critical. Tyr92 is two residues removed from the hinge on the N2 side while His253 is two residues removed on the N1 side. The hinges, thus, neatly split these two iron-binding groups, and Tyr92 moves with N2, and His253, with N1.

The movement of Tyr92 with N2 means that N2 provides four of the six iron-binding groups. Presumably, N2 serves as the site of initial binding (Anderson *et al.*, 1990). This primary role for N2 is supported by the recent structural analysis of a proteolytic fragment of duck ovotransferrin, comprising just the N2 domain (P. F. Lindley, personal communication). In this structure iron is bound to the CO_3^{2-} ion and to two tyrosine residues just as in the intact molecule. Once iron is bound to N2, the domain closure allows Asp60 and His253 to bind the iron and complete the metal co-ordination. Asp60 helps lock the two domains together with an interdomain hydrogen bond (Anderson *et al.*, 1989). The hinge motion is thus able to assemble the iron-binding site with no major impediments.

Furthermore, two simple structural observations made in the previous sections suggest that the open and closed states are similar in energy. First, the hinge has a facile nature that only requires torsion angle changes in the normally allowed region of the Ramachandran diagram. Second, because of the small interface, upon closure the exposure and burial of protein surface is more balanced than it would otherwise be. The similarity in energy of the open and closed states, in turn, implies that in solution unliganded lactoferrin exists in a dynamic equilibrium between open and closed states. Only when the iron binds is the molecule locked into a single state (Baker *et al.*, 1991). (Such an equilibrium is consistent with the closed but iron-free state of the C-lobe in apolactoferrin. It is also corroborated, albeit indirectly, by the closed but unliganded conformations that have been found for the arabinose binding protein (Sharff *et al.*, 1992, and references cited therein). As discussed in a following section, this protein is similar in structure to lactoferrin.)

The similarity in energy of the open and closed states also suggests that little energy is needed to stabilize the closed state and that the energy of the bonds to iron are primarily responsible for the very tight binding ($K_{binding} \sim 10^{20}$, Aisen & Listowsky (1980)).

7. Hinged Domain Motion in Other Proteins

Domain motion in lactoferrin involves two simple hinges and a see-saw motion between close-packed interfaces. To highlight the features of the lactoferrin mechanism that are of general relevance, it is instructive to compare its motion to other examples of hinged domain motion and then to contrast it with examples of shear domain motion.

(a) *Hinged mechanisms in the periplasmic binding proteins*

Lactoferrin has a structure similar to a number of other proteins. As pointed out previously (Baker *et al.*, 1987), the N1 and N2 domains of lactoferrin share a similar structure and topology with the group II periplasmic binding proteins, which include the sulfate, phosphate, maltodextrin, and LAO (lysine-, arginine-, ornithine-) binding proteins (Luecke & Quiocho, 1990; Pflugrath & Quiocho, 1988; Spurlino *et al.*, 1991; Kang *et al.*, 1991). The two lactoferrin domains are also similar to domains 1 and 2 of porphobilinogen deaminase (Louie *et al.*, 1992) and to the two domains in the N-terminal lobe of the transferrins (Sarra *et al.*, 1990). All the structures have ~ 300 residues in two domains, each of which has helices packed on either face of a central sheet, and two equivalent polypeptide linkages between the domains. The periplasmic binding proteins also have similarities with lactoferrin in terms of the construction of the binding site: i.e. both domains provide ligand binding groups, but one domain provides most of the groups and so serves as an initial site of attachment (Quiocho, 1990).

The maltodextrin binding protein (Sharff *et al.*, 1992; Spurlino *et al.*, 1991) has been solved in both open and closed forms. Sharff *et al.* describe the domain closure motion as a 35° rotation about an axis through the hinge region followed by an 8° rotation about a perpendicular axis. There are large and highly localized torsion angle changes in the three linkages spanning the domains. Two of these linkages are structurally equivalent to the lactoferrin hinges.

(b) *Hinged mechanisms in adenylate kinase, lysozyme, and immunoglobulins*

Hinged motions have been found in three proteins less closely related to lactoferrin than the binding

proteins: adenylate kinase, lysozyme, and the immunoglobulins. In adenylate kinase the motion about two pairs of joints on either side of two helixes enables a small domain to move up to 37 Å to cover the active site (Gerstein *et al.*, 1993; Schulz *et al.*, 1990). The 88° total rotation of this domain is considerably more than the rotation of N2 in lactoferrin and might not have been possible with only a single pair of hinges. It is divided into ~ 30° and ~ 60° rotations from each of the two pairs of hinges.

Two mutants of T4 lysozyme, Ile3 to Pro and Met6 to Ile, have domain movements (Dixon *et al.*, 1992; Faber & Matthews, 1990). Depending on which space group they crystallize in, these mutants either have structures very similar to the wild-type or differ from it by a range of rigid-body domain rotations up to 32°. These domain motions appear to be a consequence of the loss of close-packing created by the mutation. In contrast to lactoferrin, which has two hinges both located on β-strands, lysozyme has one hinge which is located on a long helix. The motion of the lysozyme hinge may have some relation to the low-frequency modes identified in normal-mode analysis (Bruccoleri *et al.*, 1986; Levitt *et al.*, 1985).

The well-known hinged domain motion in immunoglobulins presents a special case that should be carefully distinguished from that in lactoferrin. In this motion, known as "elbow motion," the V_L-V_H dimer rotates over a range of ~ 50° relative to the C_L-C_{H1} dimer. Like lactoferrin, the elbow motion involves highly localized deformations in two peptides (i.e. hinges) that link the V_L-V_H and C_L-C_{H1} dimers. However, throughout the motion the V_L-V_H dimer slides in an almost shear fashion across a continuously maintained interface with the C_L-C_{H1} dimer. This sliding motion is very different from the see-saw motion in lactoferrin. In structure, the elbow-motion interface resembles a molecular "ball-and-socket" joint (Lesk & Chothia, 1988). Because this special interface does not involve interdigitation of side-chains, it is "smooth" and facilitates a motion over a continuous range of relative orientations.

8. Conclusion: Hinge Motions *versus* Shear Motions

The hinged domain motion in lactoferrin is the structural opposite of the shear motions found in other instances of domain closure. It is worthwhile to conclude by highlighting this contrast. Shear motions are produced by the cumulative effects of several 1 to 2 Å shifts between close-packed segments of polypeptide. They are found in citrate synthase, alcohol dehydrogenase, hexokinase, trp repressor, glyceraldehyde-3-phosphate dehydrogenase, and aspartate amino transferase (Lesk & Chothia, 1984; Lawson *et al.*, 1988; Skarzynski & Wonacott, 1988; McPhalen *et al.*, 1992).

In shear motions the local motion of two elements of secondary structure, usually helices, is across and parallel to the plane of their interface. The interface itself shears. The interface side-chains usually have torsion angle changes less than 20° and retain their same packing configuration throughout the motion. They move between conformational states of nearly the same energy without crossing large energy barriers (Elber & Karplus, 1987; Rojewska & Elber, 1990; Frauenfelder *et al.*, 1991). The main-chain atoms involved in shear motions are constrained by close packing. Consequently, a shear motion is produced by small torsion angle changes spread over many angles, and the overall motion is the resultant of many small local motions.

In contrast, in the lactoferrin hinge motion, the main-chain can have large torsion angle changes in the hinges because it is free from packing constraints. The overall motion can be described as a 54° rotation about a screw axis that passes through the hinges. The rotation axes for four of the five principal torsion angle changes are roughly aligned with this screw axis, so the local changes in the hinge are clearly related to the overall motion. The overall motion is almost perpendicular to the plane of the large and small interfaces and involves the alternate exposing and burying of the two interface surfaces. The interface side-chains change conformation to some degree, but to a large extent the interfaces are preformed when open to match when closed. The packing at the base of the hinge, accomplished by Tyr92 in lactoferrin, is particularly critical.

The unconstrained main-chain atoms evident in Figure 5 are the structural signature of the hinge. If these main-chain atoms had been surrounded by tightly packed side-chains, they would not have been free to kink so sharply. Their deformation would be spread over more residues, and the hinge motion would turn into a shear motion. Consequently, both the analysis here of lactoferrin and a previous analysis of the lactate dehydrogenase loop (Gerstein & Chothia, 1991) suggest that it is possible to predict whether a particular structural element is able to move by a hinged motion by the number of steric constraints on it.

APPENDIX

Descriptions of Rigid-body Motion Useful for Studying Domain Closure

Two standard results from geometry were particularly useful in the study of protein domain movements: "screw motions" and rotational decomposition. Here they are presented in terms of simple formulae which should be immediately applicable to the analysis of protein movements. Screw motions have been used to study protein movements before but the formalism presented has been somewhat different (Colonna-Cesari *et al.*, 1986; Muirhead *et al.*, 1967). Diamond (1990) has presented a decomposition formalism for the rotations involved in diffractometry.

(a) *Screw motions*

If a set of points $\mathbf{x}$ (i.e. the atoms in a protein domain) moves as a rigid body, the transformation $\mathbf{x} \rightarrow \mathbf{x}'$ is expressible as a rotation $\mathbf{R}$ followed by a translation $\mathbf{T}$:

$$\mathbf{x}' = \mathbf{R}\mathbf{x} + \mathbf{T}.$$

Up to a sign, the rotation $\mathbf{R}$ has a unique axis $\mathbf{n}$ and magnitude κ (e.g. see Goldstein, 1980). (By convention, $\mathbf{n}$ is a normalized vector along the rotation axis, and the rotation κ is positive if it increases in a counterclockwise direction when viewed looking down $\mathbf{n}$ towards the origin.) However, the translation $\mathbf{T}$ depends on the origin of the co-ordinate system. An origin $\mathbf{x}_0$ can always be chosen (up to arbitrary translation along $\mathbf{n}$) so that the translation is parallel to the axis of rotation. Such choice of origin gives the smallest possible translation. If the initial and final co-ordinates refer to this origin, the entire transformation is referred to as a "screw motion":

$$(\mathbf{x}' - \mathbf{x}_0) = \mathbf{R}(\mathbf{x} - \mathbf{x}_0) + \mathbf{T}_\parallel,$$

where the parallel component of the translation is $\mathbf{T}_\parallel = \mathbf{n}(\mathbf{n} \cdot \mathbf{T})$, the perpendicular component is $\mathbf{T}_\perp = \mathbf{T} - \mathbf{T}_\parallel$, and the origin is:

$$\mathbf{x}_0 = \frac{1}{2}\left(\mathbf{T}_\perp + \mathbf{n} \times \mathbf{T}_\perp \cot\frac{\kappa}{2}\right).$$

(b) *Rotational decomposition*

Given a rotation $\mathbf{R}$, with axis $\mathbf{n}$ and magnitude κ, and any direction $\mathbf{n}_1$, the rotation $\mathbf{R}$ can be decomposed into a rotation $\mathbf{R}_1$ around $\mathbf{n}_1$ followed by a rotation $\mathbf{R}_2$ about an axis $\mathbf{n}_2$ perpendicular to $\mathbf{n}_1$ ($\mathbf{n}$, $\mathbf{n}_1$, $\mathbf{n}_2$ denote unit vectors). The magnitude κ_1 of rotation $\mathbf{R}_1$ is given by:

$$\tan\frac{\kappa_1}{2} = \mathbf{n}_1 \cdot \mathbf{n} \tan\frac{\kappa}{2}.$$

The perpendicular axis $\mathbf{n}_2$ and rotation angle κ_2 can then be found by expressing the axis of $\mathbf{R}_2 = \mathbf{R}\mathbf{R}_1^{-1}$ in terms of direction cosines.

M.G. acknowledges support from a Herchel-Smith Fellowship; A.M.L. acknowledges support from the Kay Kendall Foundation; and E.N.B. acknowledges support from the U.S. National Institutes of Health (grant HD-20859), the Wellcome Trust, and the Health Research Council of New Zealand.

References

Aisen, P. & Listowsky, I. (1980). Iron transport and storage proteins. *Ann. Rev. Biochem.* **49**, 357–393.

Anderson, B. F., Baker, H. M., Dodson, E. J., Norris, G. E., Rumball, S. V., Waters, J. M. & Baker, E. N. (1987). Structure of human lactoferrin at 3·2 Å resolution. *Proc. Nat. Acad. Sci., U.S.A.* **84**, 1769–1773.

Anderson, B. F., Baker, H. M., Norris, G. E., Rice, D. W. & Baker, E. N. (1989). Structure of human lactoferrin: crystallographic structure analysis and refinement at 2·8 Å resolution. *J. Mol. Biol.* **209**, 711–734.

Anderson, B. F., Baker, H. M., Norris, G. E., Rumball, S. V. & Baker, E. N. (1990). Apolactoferrin structure demonstrates ligand-induced conformational change in transferrins. *Nature (London)*, **344**, 784–787.

Anderson, C. M., Zucker, F. H. & Steitz, T. (1979). Space-filling models of kinase clefts and conformation changes. *Science*, **204**, 375–380.

Baker, E. N., Rumball, S. V. & Anderson, B. F. (1987). Transferrins: insights into structure and function from studies on lactoferrin. *Trends Biochem. Sci.* **12**, 350–353.

Baker, E. N., Anderson, B. F., Baker, H. M., Haridas, M., Jameson, G. B., Norris, G. E., Rumball, S. V. & Smith, C. A. (1991). Structure, function and flexibility of human lactoferrin. *Int. J. Biol. Macromol.* **13**, 122–129.

Bennett, W. S. & Huber, R. (1984). Structural and functional aspects of domain motion in proteins. *Crit. Rev. Biochem.* **15**, 291–384.

Bernstein, F. C., Koetzle, T. F., Williams, G. J. B., Meyer E. F., Jr, Brice, M. D., Rodgers, J. R., Kennard, O., Shimanouchi, T. & Tasumi, M. (1977). The protein data bank: a computer-based archival file for macromolecular structures. *J. Mol. Biol.* **112**, 535–542.

Brooks, B. R., Bruccoleri, R. E., Olafson, B. D., States, D. J., Swaminathan, S. & Karplus, M. (1983). CHARMM: a program for macromolecular energy, minimization, and dynamics calculations. *J. Comp. Chem.* **4**, 187–217.

Bruccoleri, R. E., Karplus, M. & McCammon, J. A. (1986). The hinge-bending mode of a lysozyme inhibitor complex. *Biopolymers*, **25**, 1767–1802.

Brünger, A. T., Kuriyan, J. & Karplus, M. (1987). Crystallographic *R* factor refinement by molecular dynamics. *Science*, **235**, 458–460.

Chothia, C. (1975). Structural invariants in protein folding. *Nature (London)*, **254**, 304–308.

Chothia, C. (1984). Principles that determine the structure of proteins. *Annu. Rev. Biochem.* **53**, 537–572.

Chothia, C. & Lesk, A. M. (1985). Helix movements in proteins. *Trends Biochem. Sci.* **10**, 116–118.

Chothia, C., Lesk, A. M., Dodson, G. G. & Hodgkin, D. C. (1983). Transmission of conformational change in insulin. *Nature (London)*, **302**, 500–505.

Colonna-Cesari, F., Perahia, D., Karplus, M., Eklund, H., Branden, C. I. & Tapia, O. (1986). Interdomain motion in liver alcohol dehydrogenase: structural and energetic analysis of the hinge bending mode. *J. Biol. Chem.* **261**, 15273–15280.

Creighton, T. E. (1984). *Proteins*, Freeman, San Francisco.

Diamond, R. (1990). On the factorization of rotations with examples in diffractometry. *Proc. Roy. Soc. ser. A*, **428**, 451–472.

Dixon, M. M., Nicholson, H., Shewchuk, L., Baase, W. A. & Matthews, B. W. (1992). Structure of a hinge-bending bacteriophage T4 lysozyme mutant, Ile3 → Pro. *J. Mol. Biol.* **227**, 917–933.

Elber, R. & Karplus, M. (1987). Multiple conformational states of proteins: a molecular dynamics analysis of myoglobin. *Science*, **235**, 318–321.

Faber, H. R. & Matthews, B. W. (1990). A mutant T4 lysozyme displays five different crystal conformations. *Nature (London)*, **348**, 263–266.

Frauenfelder, H., Sligar, S. G. & Wolynes, P. G. (1991). The energy landscapes and motions of proteins. *Science*, **254**, 1598–1603.

Gerstein, M. B. & Chothia, C. H. (1991). Analysis of protein loop closure: two types of hinges produce one motion in lactate dehydrogenase. *J. Mol. Biol.* **220**, 133–149.

Gerstein, M., Schulz, G. & Chothia, C. (1993). Domain closure in adenylate kinase: joints on either side of two helices close like neighboring fingers. *J. Mol. Biol.* **229**, 494–501.

Goldstein, H. (1980). *Classical Mechanics*, 2nd edit., Addison-Wesley, New York.

Janin, J. & Wodak, S. (1983). Structural domains in proteins and their role in the dynamics of protein function. *Prog. Biophys. Mol. Biol.* **42**, 21–78.

Kang, C.-H., Shin, W.-C., Yamagata, Y., Gokcen, S., Ames, G. F. & Kim, S.-H. (1991). Crystal structure of the lysine-, arginine-, ornithine-binding protein (LAO) from *Salmonella typhimurium* at 2·7-Å resolution. *J. Biol. Chem.* **266**, 23893–23899.

Knowles, J. R. (1991). To build an enzyme. *Phil. Trans. Roy. Soc. ser. B*, **332**, 115–121.

Kolaskar, A. S. & Kulkarni-Kale, U. (1992). Sequence alignment approach to pick up conformationally similar protein fragments. *J. Mol. Biol.* **223**, 1053–1061.

Kraulis, P. J. (1991). MOLSCRIPT—a program to produce both detailed and schematic plots of protein structures. *J. Appl. Crystallogr.* **24**, 946–950.

Lawson, C. L., Zhang, R., Schevitz, R. W., Otwinowski, Z., Joachimiak, A. & Sigler, P. B. (1988). Flexibility of the DNA-binding domains of the trp repressor. *Proteins*, **3**, 18–31.

Lee, B. & Richards, F. M. (1971). The interpretation of protein structures: estimation of static accessibility. *J. Mol. Biol.* **55**, 379–400.

Lesk, A. M. (1991). *Protein Architecture: A Practical Approach*, IRL Press, Oxford.

Lesk, A. M. & Chothia, C. (1984). Mechanisms of domain closure in proteins. *J. Mol. Biol.* **174**, 175–191.

Lesk, A. M. & Chothia, C. (1988). Elbow motion in the immunoglobins involves a molecular ball and socket joint. *Nature (London)*, **335**, 188–190.

Levitt, M. & Chothia, C. (1976). Structural patterns in globular proteins. *Nature (London)*, **261**, 552–558.

Levitt, M., Sander, C. & Stern, P. S. (1985). Protein normal-mode dynamics: trypsin inhibitor, crambin, ribonuclease, and lysozyme. *J. Mol. Biol.* **181**, 423–447.

Louie, G. V., Brownlie, P. D., Lambert, R., Cooper, J. B., Blundell, T. L., Wood, S. P., Warren, M. J., Woodcock, S. C. & Jordan, P. M. (1992). Structure of porphobilinogen deaminase reveals a flexible multidomain polymerase with a single catalytic site. *Nature (London)*, **359**, 33–39.

Luecke, H. & Quiocho, F. A. (1990). High specificity of a phosphate-transport protein determined by hydrogen-bonds. *Nature (London)*, **347**, 402–406.

McPhalen, C. A., Vincent, M. G., Picot, D., Jansonius, J. N., Lesk, A. M. & Chothia, C. (1992). Domain closure in mitochondrial aspartate aminotransferase. *J. Mol. Biol.* **227**, 197–213.

Mowbray, S. L. (1992). Ribose and glucose-galactose receptors. Competitors in bacterial chemotaxis. *J. Mol. Biol.* **227**, 418–440.

Muirhead, H., Cox, J. M., Mazzarella, C. & Perutz, M. F. (1967). Structure and function of haemoglobin III. A three-dimensional Fourier synthesis of human deoxyhaemoglobin at 5·5 Å resolution. *J. Mol. Biol.* **28**, 117–156.

Norris, G. E., Anderson, B. F. & Baker, E. N. (1991). Molecular replacement solution of the structure of apolactoferrin, a protein displaying large-scale conformational change. *Acta Crystallogr. sect. B*, **47**, 998–1004.

Pflugrath, J. W. & Quiocho, F. A. (1988). The 2 Å resolution structure of the sulfate-binding protein involved in active-transport in *Salmonella typimurium*. *J. Mol. Biol.* **200**, 163–180.

Ponder, J. W. & Richards, F. M. (1987). Tertiary templates for proteins: use of packing criteria in the enumeration of allowed sequences for different structural classes. *J. Mol. Biol.* **193**, 775–791.

Quiocho, F. A. (1990). Atomic structures of periplasmic binding proteins and the high-affinity active transport systems in bacteria. *Phil. Trans. Roy. Soc. ser. B*, **326**, 341–351.

Richards, F. M. (1974). The interpretation of protein structures: total volume, group volume distributions and packing density. *J. Mol. Biol.* **82**, 1–14.

Richards, F. M. (1979). Packing defects, cavities, volume fluctuations, and access to the interior of proteins. including some general comments on surface area and protein structure. *Carlsberg. Res. Commun.* **44**, 47–63.

Rojewska, D. & Elber, R. (1990). Molecular dynamics study of secondary structure motions in proteins: application to myohemerythrin. *Proteins*, **7**, 265–279.

Sarra, R., Garratt, R., Gorinsky, B., Jhoti, H. & Lindlay, P. (1990). High-resolution X-ray studies on rabbit serum transferrin – preliminary structure analysis of the N-terminal half-molecule at 2·3 Å resolution. *Acta Crystallogr. sect. B*, **46**, 763–771.

Schulz, G. E., Muller, C. W. & Diederichs, K. (1990). Induced-fit movement in adenylate kinases. *J. Mol. Biol.* **213**, 627–630.

Sharff, A. J., Rodseth, L. E., Spurlino, J. C. & Quiocho, F. A. (1992). Crystallographic evidence of a large ligand-induced hinge-twist motion between the two

domains of the maltodextrin binding protein involved in active transport and chemotaxis. *Biochemistry*, **31**, 10657–10663.

Skarzynski, T. & Wonacott, A. J. (1988). Coenzyme-induced conformational changes in glyceraldehyde-3-phosphate dehydrogenase from *Bacillus stearothermophilus*. *J. Mol. Biol.* **203**, 1097–1118.

Spurlino, J. C., Lu, G. Y. & Quiocho, F. A. (1991). The 2·3 Å resolution structure of the maltose-binding or maltodextrin-binding protein, a primary receptor of bacterial active-transport and chemotaxis. *J. Biol. Chem.* **266**, 5202–5219.

Edited by B. Honig